CO_2 capture in biocompatible amino acid ionic liquids: exploring the reaction mechanisms for bimolecular absorption processes.

Stefano Onofri [a,b] and Enrico Bodo [a]*

[a] Department of Chemistry, University of Rome "La Sapienza", Piazzale A. Moro 5, 00185, Rome, Italy;

[b] Faculty of Engineering Technology, Institute for Nanotechnology, University of Twente, Enschede 7500 AE, The Netherlands

ABSTRACT

CO_2 capture at the production site represents one of the accessible ways to reduce its emission in the atmosphere. In this context, CO_2 chemisorption is particularly advantageous and is often based on exploiting a liquid containing amino groups that can trap CO_2 due their propensity to react with it to yield carbamic derivatives. A well-known class of ionic liquids based on amino acids anions might represent an ideal medium for CO_2 capture because, at difference with present implementations, they are known to be fully biocompatible. One of the problems is however the relatively low molar ratio of CO_2 absorption. Increasing this ratio turns out to be possible by choosing appropriate anions. We present here a set of accurate computations to elucidate the possible reaction paths that allow the anion to absorb two CO_2 molecules, thus effectively doubling the overall intake. An extensive exploration of some reaction mechanisms suggests that some of them might be quite efficient even under mild conditions.

[*] Corresponding author: E-mail: enrico.bodo@uniroma1.it

1   Introduction

The increase in CO_2 emission by anthropic activities represent one of the most serious threats for the ecosystem as it represents the main source of worldwide temperature increase [1–3]. Since the majority of CO_2 emissions are due to fossil fuels processing [4] and, specifically, more than half of these come from power plants, part of the overall research effort has been devoted to finding economic and environmentally friendly ways to capture and remove CO_2 from flue gases at the production sites. [5–7] One of the present capture techniques is based on chemisorption and, in particular, on exploiting the chemical reaction of CO_2 with amines. [8,9] These technologies, however, are currently based on corrosive and harmful aqueous amine solutions and represent expensive and non-ecofriendly approaches. [10]

Ionic liquids (ILs) have been proposed as an alternative to aqueous amines solutions for CO_2 capture since the early years of the past decade [11] and the study of these task-specific ILs is, at the moment, a very active field of research recently summarized in previous reviews. [12–15]. The typical advantage of ILs over other solvents lie in their negligible vapor pressure and in their tunable chemical composition which allows them to be optimized for specific tasks. [16,17] CO_2 absorption by ILs can be achieved by both physisorption and chemisorption, with the latter often having a greater efficiency. CO_2 chemisorption can be realized by inserting amino groups in their molecular components to allow their reaction with CO_2 to form carbamates or carbamic acids. [18–23]

Among the ILs specifically synthetized for CO_2 chemisorption, those based on anions made by a deprotonated amino acid (AA) [24,25] seem to yield a positive balance between absorption capacity, synthetic cost and biocompatibility [26–28]. In these ILs, CO_2 absorption occurs to various extents depending on the physical conditions and on their molecular components, from 0.5 mol of CO_2 per mol of IL (1:2 mechanism), to 1 mol of CO_2 per 1 mol of IL (1:1 mechanism) and to even higher molar fractions (2:1 mechanisms). [21,22,29,30]

The general reaction scheme of CO_2 with amines is known [31,32] and consists in the two-reactions process (R1) reported in Scheme 1. If the second reaction takes place, the absorption process is typically characterized by an overall 1:2 stoichiometry, hence by a low efficiency since two AA anions are used to incorporate only one CO_2 molecule. Instead, if the second reaction is inefficient or hindered, the overall absorption process proceeds with a 1:1 stoichiometry. If a second attack by another CO_2 molecule is possible (either on the residual NH group of the AA anion, or on

another –NH$_2$ group of the same anion) the final stoichiometry tends to a 2:1 molar ratio. It is obvious that, to promote efficiency, it would be desirable to reach the latter situation.

$$-NH_2 \ + \ CO_2 \ \longrightarrow \ -NHCO_2H$$
$$-NHCO_2H \ + \ -NH_2 \ \longrightarrow \ -NHCO_2^- \ + \ -NH_3^+$$

(R1)
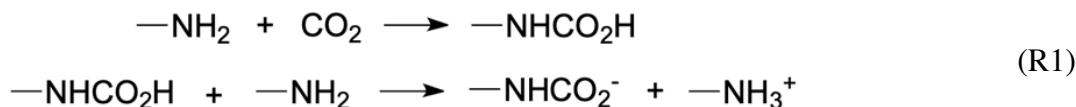
Scheme 1: general reaction process of CO_2 with the –NH$_2$ group.

The CO_2 addition (first reaction of R1) can be further divided into the three steps [33] shown in Scheme 2: the initial one is the formation of a pre-reaction complex with zwitterionic character followed, in step 2, by a proton transfer (PT) from the positive nitrogen to one of the carboxylates. The final product is represented by the most stable of the two possible tautomeric forms which can interconvert via further inter- or intra-molecular PTs (step 3).

(R2)
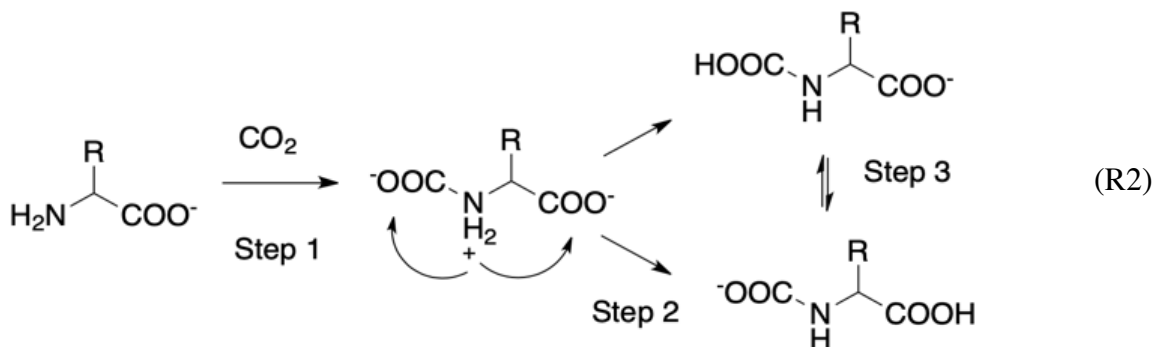
Scheme 2: The general reaction between an AA anion and a first molecule of CO_2. In the first step a zwitterionic pre-reaction complex is formed. A subsequent PT (step 2) removes the zwitterion and forms a carbamic acid derivative or a carbamate depending on the preferential site of PT. An isomerization equilibrium can then take place (step 3).

Several computational descriptions of this mechanism have appeared in the literature, [34–39] and have been summarized in a review by Sheridan et al.. [40] More recently, we have explored the absorption mechanisms of a single CO_2 molecule by different prototypical AA anions. [32] Overall, the features of R2 can be summarized as follows:

1. The efficiency in the formation of the pre-reaction complex is limited by the diffusion of CO_2 in the liquid and by the energy necessary to "desolvate" the amino group and make it available for the reaction. The latter can be considered as the energy required to break the ionic couple in which the anion is bound. [35] This explains why the high viscosity of these fluids is an issue and, at the moment, a key factor that severely limits their practical usability. [41,42]

2. Once the CO_2 molecule is able to attack the $-NH_2$ group, the ensuing reaction toward the carbamic AA derivative is almost invariably exothermic hence thermodynamically favored. The rate limiting step is the PT from the nitrogen to the carboxylate to form the AA anion carbamic derivative. Owing to interionic Coulomb repulsion, the PT is more likely to occur within the same molecule rather than between two different anions. In principle, the kinetic of the reaction is therefore determined by the energy barrier along the PT step, but we have recently shown that, depending on the nature of the AA, there exist reactive pathways with null or negligible activation barriers. [32]

3. The formation of the primary AA carbamic derivative can be followed by additional isomerization reactions to form other isomers, depending on which structure is more stable.

One of the problems which has been only seldom explored in previous works [43,44] is why some of the liquids based on AA anions present molar absorption intakes (2:1 mechanism) which are larger than one. On the one hand, it is obvious that AA anions such as [Lys]⁻ that have two $-NH_2$ groups allows for molar intakes larger than 1 thanks to the double reaction sites (for [Lys]⁻ a molar ratio of 1.6 has been measured [43,45]). On the other hand, ILs based on simple AA anions such as [Gly]⁻ (with a molar ratio of 1.2 [46]) or doubly deprotonated ones such as [Asp]²⁻ (with molar ratio ~2 [43]) clearly present the ability of incorporating, at least partially, a second CO_2 molecule, albeit in a less obvious way.

It is the purpose of this work to explore via ab-initio calculations the mechanism at the basis of these experimental results using four different prototypical AA anions: [Gly]⁻, [Asp]²⁻, [Lys]⁻ and [DAP]⁻ (2,3-diaminopropionate), a smaller analogue of [Lys]⁻. Their structures are shown in Scheme 3.
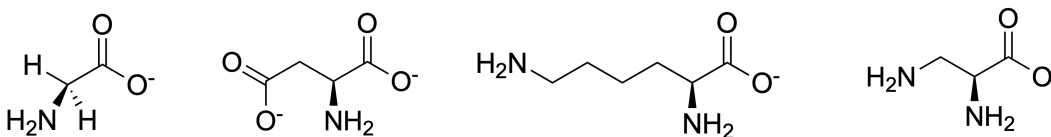
Scheme 3: Structures of the 4 AA anions used in this work: from left to right, glycinate, doubly deprotonated aspartate, lysinate and 2,3-diaminopropionate.

In order to maintain generality, we have to simplify the overall problem to make the results independent of the many variables at play. First of all, in the framework of ab-initio calculations, we are unable to account for the presence of an explicit surrounding liquid. In ref. [32] we have taken into account the environmental effects using the PCM approximation using the parametrization for a solvent with a medium dielectric constant (35). The results indicate that the presence of such environment does not alter significantly the overall reaction profiles with only minor variations of the PT barrier. The main effect of the surrounding dielectric medium is a reduction of the reactant-to-product energy difference (ΔH of reaction). This is simply due to the condensation nature (A+B $\rightarrow$C) of the present reactions. A dielectric medium induces a greater stabilization of the bimolecular reactants than of the final product because of the appearance of two solvation shells in the A+B channel. Given this situation, we have decided here to focus our discussion mainly on gas-phase results, but we will present also continuum model solvation results for reference.

In order to make our calculations independent of the peculiarities of the actual liquid and to provide a general mechanism, we will not include a cationic partner. While the nature of the cation in the reaction has been proven, in certain conditions, to be relevant, [30,47] to correctly address its role within the present context and within our computational approach is not easy since, in an isolated system, is arguably very different from the one it can play in the actual bulk phase of ILs. In other words, apart from the case in which the cation partakes to the absorption reaction because it possesses amino groups, its role can emerge because it influences the structural and frictional properties of the fluid, e.g., the diffusion of CO_2 in it. Such many body effects are however precluded to our present investigation and, it would be difficult to ascertain the peculiar effects due to cations. In addition, the study reported by Shaikh et al. [39] indicates how, using a computational approach based on isolated ionic couples, the effect of different weakly coordinating cations (such as those typically used in ILs) can be relatively unimportant in modifying the reaction profile of the [Gly]$^-$ anion (compare Figures 2 and 3 of the cited work). That the effect of the cation choice on the reaction profile can be small is also seen in the rather extensive data reported by Firaha and Kirchner [35] and, in particular, in the reported energies associated with the proton transfer step (Table S2 in the cited paper) that show significant variations among the AA anions but change only slightly for cation variations.

Finally, the study of the influence of the cationic partner on the reaction mechanisms would require a complete, systematic study of its role as a function of its coordinating properties, size and steric shape. This task, albeit worth undertaking, lies well outside the scope of the present treatment which aims at the characterization of the reaction profile of the unperturbed anions. We believe that the exploration of the reaction mechanisms of the anions alone (an approach that has its limits but is at least universal for all AA based ILs) represents a prerequisite for further studies: on the one hand, our simplified approach eases the interpretation of the peculiar experimental evidence for specific ILs and, on the other, helps in setting the starting point for possible future theoretical studies in more specific conditions.

2   Computational Methods

The ab-initio calculations have been carried out for the isolated reagents, i.e. the AA anion plus CO_2 (**R**), for the pre-reaction complex (**CR**) and for the products (**P**). Since the formation of **CR** from **R** is barrierless, the dominant transition state (**TS**) has been localized between **CR** and **P**. When the product **P** presents more than one tautomeric or isomeric structure, we will report only the one with the lowest energy. For each structure, we have performed an unconstrained optimization and evaluated the harmonic frequencies using the dispersion-corrected B3LYP-D3 functional [48] with the 6-311+G(d,p) basis set. All minima and saddle points have been verified by computing the full hessian and by checking the relative vibrational frequencies. When needed, we have made sure the uniqueness of the transition state by computing the IRC, but we will not report these consistency-check calculations. The computational model has been previously verified as accurate enough when compared to CBS-QB3 and G4MP2 composite methods [32]. The Gaussian16 [49] package was used for all the ab-initio calculations. We have included the zero-point-energies in all the energetic values reported in the rest of the paper. Regarding the harmonic analysis, we should point out that, even though it provides a value for the Gibbs free energy, its calculation is based on the perfect gas model and cannot be considered as entirely accurate for a liquid environment where the rotational and translational degrees of freedom are hindered.

The presence of a surrounding medium has been evaluated by repeating the calculations in a continuum SMD [50] solvent model with the parameters of acetonitrile which has a dielectric constant of 35 which is only slightly greater than that of AA based ILs. [51] This choice should ensure that we are including in our calculations a sufficient dielectric screening to induce a stabilization

of charge separated species and mimicking the dielectric response (albeit in slight excess) of the surrounding IL.

3   Results and discussion

3.1 The prototype: the glycinate anion

We have already presented the mechanism of the reaction of glycinate with the first CO_2 molecule in ref. [32]. The initial zwitterionic complex can evolve through two possible pathways that lead to the formation of the carbamic derivative. The proton transfer transition states are characterized by a cyclic structure with 4 or 5 atoms in the ring. Only the one with a 5-member ring (owing to the minor strain) is viable and has a low barrier with respect to the zwitterionic complex (2.2 kcal/mol in terms of free energy). This pathway is certainly the one that allows the absorption of the first CO_2 molecule. The resulting carbamate derivative of the AA anion is now the reagent **R** of the reaction with the second CO_2 molecule.

The first route toward the second CO_2 molecule absorption (PT2-4) is described by the geometries of the stationary points reported in the top sequence of Figure 1 and by the corresponding energies in Table 1. The initial reagent is the glycinate carbamate derivative **R**, in Figure 1 that is the most stable tautomer of this anion. It shows only a small propensity to bind a second CO_2 molecule that, in this case, forms only a relatively weak complex (**CR**) with ~5 kcal/mol of binding energy. The O_2C-N distance in the weak pre-reaction complex is 2.8 Å and no charge transfer has been detected with the CO_2 remaining neutral. The insertion of CO_2 into the molecule costs energy and takes place simultaneously to the proton transfer from the nitrogen to the newly formed carboxyl (**TS**). The cycle has 4 members and is heavily strained with a C-N-H angle of 70°, hence its energy is ~40 kcal/mol above **CR**. This path is clearly completely precluded at low temperatures.

A second reactive path is available to [Gly]⁻ that does not involve a CO_2-AA complex, but requires a low energy isomerization of the carbamic derivative. This path, called PT2-i is illustrated in the bottom sequence of Figure 1 and the energies of the overall reaction are reported in Table 1. The starting point is the same of PT2-4, i.e., the glycinate carbamate derivative **R**. It isomerizes to **R$_i$**. that is a carbamic acid. The latter, in turn, passes through a cyclic transition state (**TS**) and isomerizes again into the structure **P$_1$** which has a negatively charged (-0.5e) —N—

group. The isomerization from R_i to P_1 costs ~15 kcal/mol overall (~16 kcal/mol in the solvent model) and the energy of TS and of P_1 is essentially the same within ~0.1-0.3 kcal/mol. Compound P_1 is a short lived intermediate whose final reaction with the CO_2 molecule (not shown) is barrierless and exoergic and leads to the same final compound P of PT1-4.
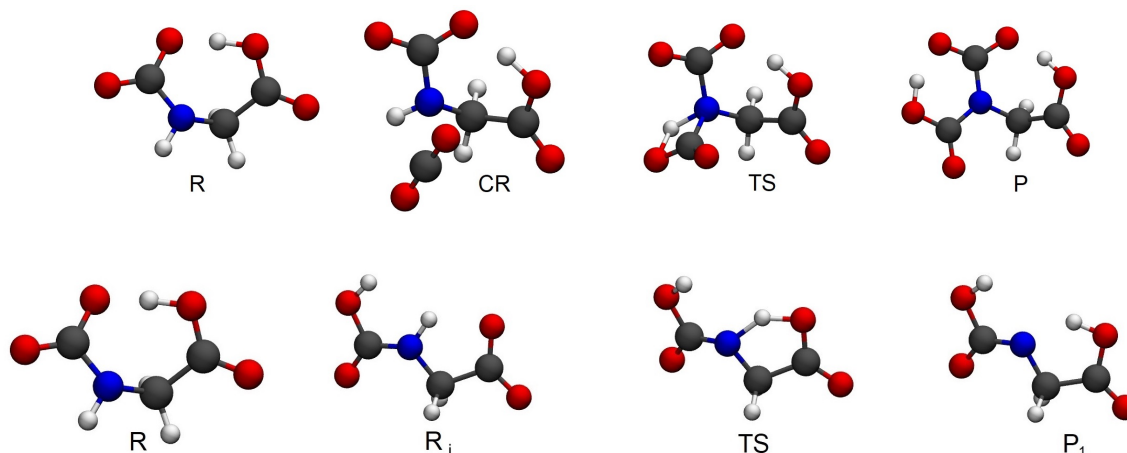

Figure 1: Geometries involved in the addition of a second CO_2 molecule to the glycinate anion along the PT2-4 path (top) and PT2-i one (bottom). The final reaction of P_1 with CO_2 is not shown, but it directly leads to compound P on top.

Table 1: Energies (at 300 K) for the second CO_2 molecule insertion in the glycinate anion through the PT2-4 and PT2-i mechanisms in kcal/mol. The reference energy is R i.e., the [Gly]$^-$ carbamate derivative plus an isolated CO_2 molecule (see Figure 1). The value in parenthesis have been obtained using the SMD solvation model.

Step	Δ(E+ZPE)	ΔH	ΔG
Mechanism PT2-4			
R→P	-12.22 (-5.23)	-13.05 (-6.09)	-1.60 (+5.50)
CR→TS	+39.45 (+41.43)	+38.45 (+40.43)	+42.98 (+43.48)
Mechanism PT2-i			
R→[P₁]→P	-12.22 (-5.23)	-13.05 (-6.09)	-1.60 (+5.50)
R→Rᵢ	+9.03 (+6.14)	+9.50 (+6.63)	+7.99 (+5.17)
Rᵢ→TS ~ [P₁]	+5.44 (+10.75)	+5.01 (+10.30)	+6.10 (+11.34)

Both the mechanisms PT2-4 and PT2-i are globally exoergic/exothermic of about 12-13 kcal/mol, a value which is reduced in a solvent model to ~6 kcal/mol because of the greater stabilization of the reactants R (two individually solvated molecules) with respect to the product P (one molecule). The entropic contribution in passing from two molecule to one is obviously negative and reduces the overall free energy gain of the reaction to -1.6 kcal/mol in vacuo and to +5.5 kcal/mol in a solvent model, but, as we mentioned above, the entropy contribution could be overestimated due to being computed in the perfect gas approximation. Kinetically, PT2-i is far more efficient than

PT2-4 since the former has an overall barrier of about 14 kcal/mol (instead of ~40) which is not prohibitive even at room temperature. The appearance of the PT2-i mechanism in liquids containing the glycinate anion might explain why the overall CO_2 intake exceeds 1.

3.2   Multiple amino groups: Lys and DAP

A double intake of CO_2 in AA-based ILs can simply take place because the anion has two amino groups available for attack by CO_2. Both [Lys]- and [DAP]- have this kind of structure.
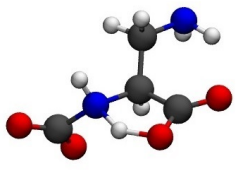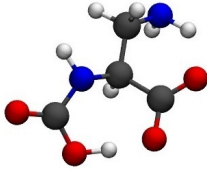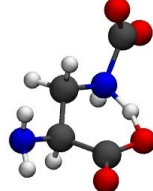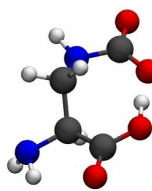
We begin by looking at the DAP anion which is an AA with a- CH_2NH_2 side chain. The reaction with the first CO_2 molecule takes place following the mechanisms detailed in our previous work [32] and illustrated in Scheme 2. The first option (PT1-5) sees the CO_2 attack on the NH_2 of the AA, the second one (PT1-6) has the CO_2 attacking the NH_2 group of the side chain. This obviously leads to two different final products.

In PT1-5 the reaction is activated by the initial formation of the zwitterionic complex **CR** (see Scheme 2) where the O_2C-N distance is 1.7 Å, the charge of the NH_2 group is +0.3e and that of CO_2 is -0.4e. The **TS** structure is characterized by a 5-member cycle (see Table 2) where the N—H and H—O distances are 1.3 and 1.2 Å respectively. The proton transfer produces a carbamate that evolves toward the final product **P** which is a carbamic acid derivative with an intramolecular O—H—O hydrogen bond with an O—O distance of 2.5 Å.

Analogously, the PT1-6 mechanism initiates from a zwitterionic complex **CR** with a O_2C-N distance of 1.7 Å, a +0.2e charge on NH_2 and a -0.5e one on CO_2. The **TS** structure is characterized by a 6-member cycle (see Table 2) where the N—H and H—O distances are 1.3 and 1.2 Å respectively. The final product in this mechanism is directly the carbamate anion derivative **P**.

The overall energetic balance and reaction barriers are summarized in Table 2. The reactions are exothermic/exoergic and proceed with a small activation barrier of 2-3 kcal/mol for PT1-5 and no barrier for PT1-6. Both processes are very effective in incorporating CO_2 in the liquid. The inclusion of solvent effects does not change much this picture: exothermicity is slightly reduced, but the activation barrier is substantially unaffected.

Table 2: Energies (at 300 K) for the [DAP]$^-$ reaction with the first CO_2 molecule along the PT1-5 and PT1-6 mechanisms in kcal/mol. The reference energy is **R**, that is [DAP]$^-$ and an isolated CO_2 molecule. The transition state and product structures are also shown. The values in parenthesis come from the inclusion of a solvent model.

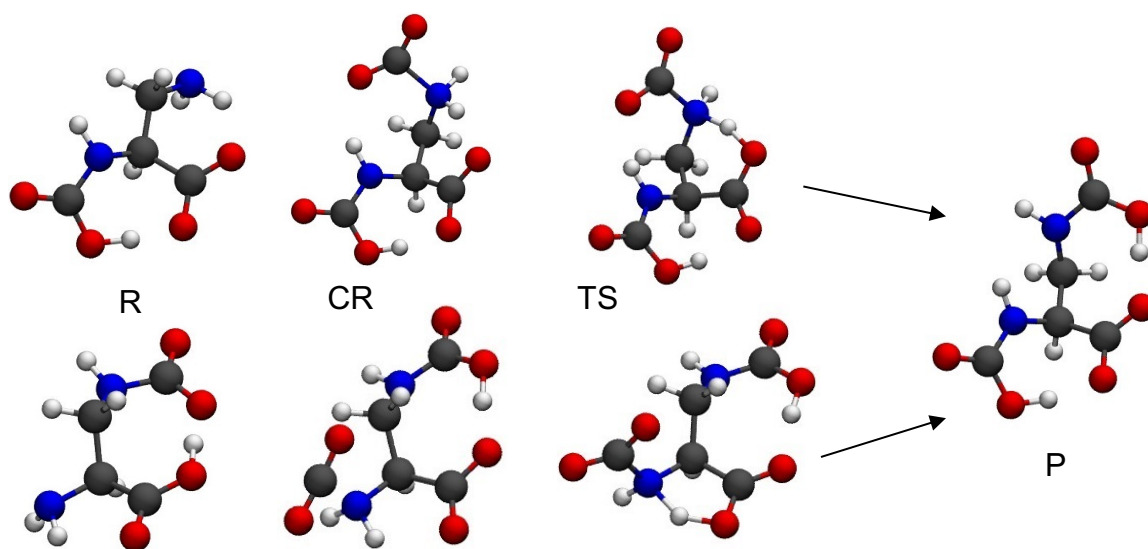| Step	Δ(E+ZPE)	ΔH	ΔG	TS	P
Mechanism PT1-5					
R→P	-17.00 (-12.94)	-17.99 (-14.00)	-6.00 (-1.74)		
CR→TS	+2.30 (+2.59)	+1.86 (+2.24)	+3.12 (+3.26)		
Mechanism PT1-6					
R→P	-14.67 (-12.43)	-15.51 (-13.35)	-4.20 (-1.97)		
CR→TS	-0.71 (-0.82)	-1.11 (-1.21)	-0.04 (+0.10)		

Figure 2: Geometries involved in the addition of a second CO_2 molecule to the DAP anion. Top sequence: PT2-6, bottom one: PT2-5.

Starting from the two structures reported in Table 2 on the right, we have analyzed the two possible further attacks of CO_2 on the surviving NH_2 groups. The sequences of structures are reported in Figure 2. The top sequence (PT2-6) begins with the product of PT1-5 and evolves through an initial zwitterionic complex (**CR**) and a 6-member **TS** toward the final **P** product. The **CR** complex is characterized by a O_2C—N distance of 1.7 Å, a net charge of +0.2 on NH_2 and -0.4e on CO_2. The transition state is a 6-member ring with N—H and O—H distances of 1.3 and 1.2 Å respectively. The final product is an anion with two protonated carbamic acid groups.

The bottom sequence (PT2-5) starts with the product of PT1-6, evolves with a weakly bound **CR** complex, passes through a 5-member ring **TS**, and yields the same product **P**. The pre-reaction complex has no zwitterionic character with a neutral CO_2 molecule weakly bound to the NH_2 at 2.7 Å. The transition state has a 5-member ring with N—H and O—H distances in line with the previously described analogous structures.

Table 3: Energies (at 300 K) in kcal/mol for the second CO_2 molecule insertion in [DAP]$^-$ along the PT2-5 and PT2-6 mechanisms (see Figure 2). The reference energy is **R**, that is the [DAP]$^-$ carbamate derivative anion plus an isolated CO_2 molecule. The value in parenthesis have been obtained using the SMD solvation model.
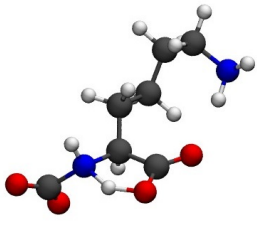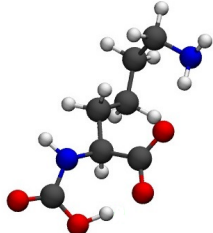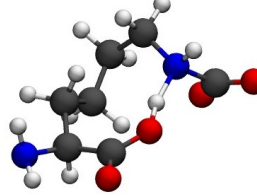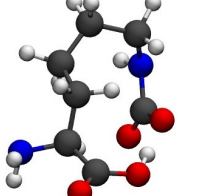
Step	Δ(E+ZPE)	ΔH	ΔG
Mechanism PT2-5			
R→P	-12.55 (-9.93)	-13.53 (-10.95)	-1.35 (+1.31)
CR→TS	+9.85 (+8.36)	+8.55 (+7.00)	+13.62 (+11.07)
Mechanism PT2-6			
R→P	-10.22 (-9.42)	-11.04 (-10.30)	+0.45 (+1.12)
CR→TS	+0.03 (+1.62)	-0.5 (+1.17)	+1.08 (+2.55)

The energetic features of the PT2-5 and PT2-6 pathways are summarized in Table 3. The PT2-5 mechanism is exothermic/exoergic and remains so in terms of free energy despite the unfavorable entropy changes due to passing from two to one molecule. A barrier of about ~10 kcal/mol is present and affects the PT step, but the process is nevertheless possible at room temperature. The PT2-6 pathway is also endothermic and not hindered by a significant activation barrier. The latter seems to appear as a very efficient route for the insertion of the second CO_2 molecule. The calculations including the solvent effect further confirm the existence of this second exothermic pathway with no activation barrier (PT2-6).

The lysinate anion behaves in a somewhat analogous way to [DAP]$^-$. The side chain is much longer having 4 methylene groups. The first CO_2 molecule inserts itself in an analogous way as in [DAP]$^-$. We have identified two viable mechanisms which resemble the PT1-5/6 ones for [DAP]$^-$. They are both illustrated in Table 4. In PT1-5 the attack is on the AA NH_2 group and the **TS** has a 5-member ring, while in PT1-9 the attack is on the NH_2 of the side chain with a **TS** with a 9-member ring. Both mechanisms begin with the formation of a zwitterionic **CR** complex which shares the same features of the one we have seen for [DAP]$^-$. The only relevant difference with DAP is that the PT1-9 pathway has a "late" transition state where the proton is already near the oxygen with the O—H distance being 1.1 Å and the N—H one 1.4 Å.

Both reactions are exothermic both in vacuo and in the solvent model and are characterized by low activation barriers (~4 kcal/mol of free energy). Once again, the presence of a solvent medium manifests itself through an overall reduction of the exothermicity of the reaction but has little or no effects on the activation barrier of the process.

Table 4: Energies (at 300 K) for the [Lys]$^-$ reaction with the first CO_2 molecule along the PT1-5 and PT1-9 mechanisms in kcal/mol. The reference energy is **R**, that is [Lys]$^-$ plus an isolated CO_2 molecule. The transition state and product structures are also shown. The value in parenthesis have been obtained using the SMD solvation model.

Step	Δ(E+ZPE)	ΔH	ΔG	TS	P
Mechanism PT1-5					
R→P	-17.36 (-13.64)	-18.26 (-14.60)	-6.22 (-2.78)		
CR→TS	+2.92 (+2.73)	+2.48 +2.42)	+3.68 (+3.10)		
Mechanism PT1-9					
R→P	-16.32 (-13.40)	-17.26 (-14.34)	-4.68 (-2.28)		
CR→TS	+2.75 (+2.72)	+2.15 (2.26)	+4.01 (+4.04)		

The two products from PT1-5 and PT1-9 are different molecules that can react with a second CO_2 molecule. The molecule resulting from the PT1-9 can undergo a second attack on the AA amino group and incorporate the second CO_2 molecule in as much the same way as in the PT2-5 mechanisms of [DAP]$^-$. The PT transfer is, as usual, the rate determining step in this reaction: it can involve either the nearest carboxyl or the farthest one. It turns out that, in analogy with PT2-5 for [DAP]$^-$, the former has a sizable activation barrier (~6-7 kcal/mol), while the latter has a negligible one. This mechanism (PT2-10a) is therefore particularly efficient since it is also exothermic of about ~18 kcal/mol and it is illustrated in Figure 3 (top sequence). The geometric features of this mechanisms are not dissimilar from those already described for [DAP]$^-$ and we shall not repeat them here.

The carbamate derivative of lysinate coming from PT1-5 can also undergo a second CO_2 addition at the NH$_2$ on the side chain through a mechanism that we call PT2-10b and is reported in Figure

3 (bottom sequence). The final product is the same as that produce by the PT2-10a path. This path is however hindered by a very large activation barrier of ~35 kcal/mol and is therefore highly inefficient.
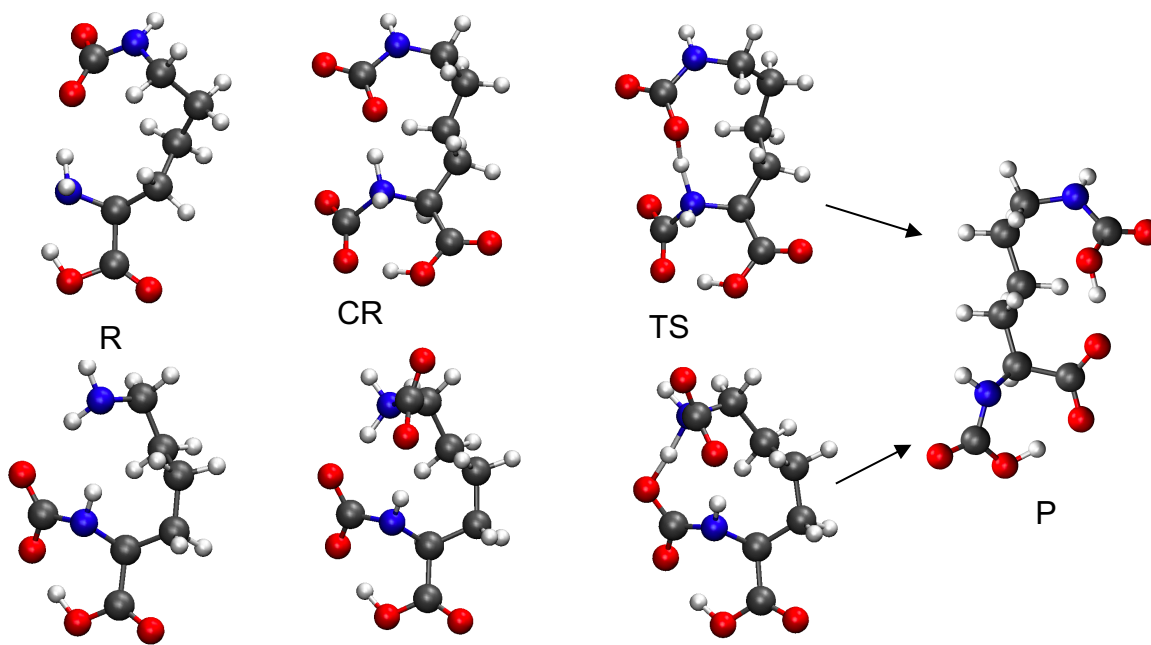

Figure 3: Geometries involved in the addition of a second CO_2 molecule to the carbamate derivative of the Lys anion. Top sequence: PT2-10a, bottom one: PT2-10b.

3.3   Doubly deprotonated AA: the dianion of Asp

Ionic liquids based on the doubly deprotonated aspartate anion have been found to absorb CO_2 with a 2:1 mechanism. The first molecule of CO_2 enters via the two mechanisms PT1-5 and PT1-6 seen for other AA anions and reported by us in ref. [32] These paths resemble the two found for the DAP anion, but in this case the final product is only one because there is only one NH_2 group. The details and relevant geometries are in Table 5. Both reactions are exothermic/exoergic, and the PT1-6 path has a negligible barrier (~0-2 kcal/mol), hence the high absorption efficiency of this anion. The PT1-5 and PT1-6 mechanisms begin with the formation of the same zwitterionic complexes **CR** that is characterized by an O_2C-N distance of 1.6 Å. The zwitterionic character is here enhanced with respect to the previous cases with a charge of +0.4 on NH_2 and -0.6 on CO_2. The final product **P** is a carbamate derivative with the residual proton on the aminoacid

carboxylate. The structure is stabilized by a strong intramolecular hydrogen bond with a O—O distance of 1.4 Å.

A second molecule of CO_2 can also be inserted into the resulting carbamate (**P** in Table 5) exploiting the PT2-4 mechanism that we have already seen for the glycinate anion that involves a 4-member ring proton transfer. As for glycinate, however, the PT2-4 mechanism is hindered by a ~30 kcal/mol barrier which renders it impossible at room temperature. The additional flexibility of the $[Asp]^{2-}$ anion with respect to glycinate allows for two more paths to incorporate the second CO_2 molecule. We have found two very similar mechanisms that differ for the number of atoms involved in the ring of the cyclic transition state during PT. The energetic and the relevant structures are reported in Table 6. For both mechanisms the starting reagent is the **P** molecule of Table 5 and the final product is the same. The reaction is exothermic albeit only slightly in a solvent medium. Both mechanisms have average to low activation barriers of less than 10 kcal/mol (in terms of free energy) and justifies the ability of this anion to bind two CO_2 molecules. The geometric features of the structures involved (such as N—H and O—H distances in **TS**) are not dissimilar from what has been previously found for the other ions.

Table 5: Energies (at 300 K) for the Asp^{2-} reaction with the first CO_2 molecule along the PT1-5 and PT1-6 mechanisms in kcal/mol. The reference energy is **R**, that is the Asp^{2-} anion plus an isolated CO_2 molecule. The transition state and product structures are also shown. The value in parenthesis have been obtained using the SMD solvation model.
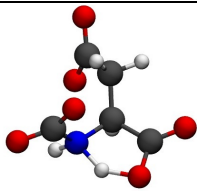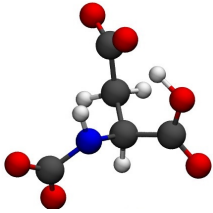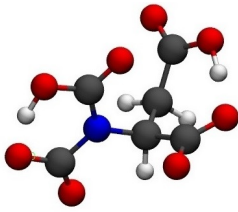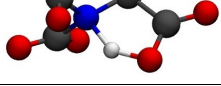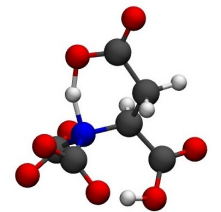
Step	Δ(E+ZPE)	ΔH	ΔG	TS	P
Mechanism PT1-5					
R→P	-26.07 (-14.33)	-26.91 (-15.27)	-15.29 (-3.52)		
CR→TS	+4.82 (+6.00)	+4.51 (+5.75)	+4.94 (+6.06)		
Mechanism PT1-6					
CR→TS	+1.22 (-0.27)	+0.78 (-0.62)	+1.90 (+0.21)		

Table 6: Energies (at 300 K) for the $[Asp]^{2-}$ reaction with the second CO_2 molecule along the PT2-5 and PT2-6 mechanisms in kcal/mol. The reference energy is **R**, that is the carbamate derivative of the $[Asp]^{2-}$ anion (**P** in Table

5) plus an isolated CO_2 molecule. The transition state and product structures are also shown. The value in parenthesis have been obtained using the SMD solvation model.
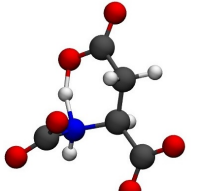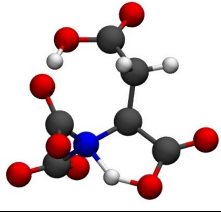
Step	Δ(E+ZPE)	ΔH	ΔG	TS	P
Mechanism PT2-5					
R→P	-13.50 (-3.74)	-14.37 (-4.57)	-2.14 (+7.55)		
CR→TS	+5.22 (+3.56)	+4.71 (+3.12)	+6.36 (+4.56)		
Mechanism PT2-6					
CR→TS	+5.40 (+8.06)	+4.24 (+6.78)	+7.89 (+10.98)		

4   Conclusions

In this paper we have examined the possible absorption mechanisms of two CO_2 molecule by a selected set of prototypic AA anions. The calculations (in vacuo) show that for all the anions there exist possible mechanisms that are viable at room temperature for a double intake of CO_2.

The first CO_2 molecule is incorporated in the anion through a reaction with the $—NH_2$ group that transform the AA anion into a carbamic derivative. AA anions with an additional $—NH_2$ group can easily react with a second CO_2 molecule and we have shown that both lysinate and diaminopropionate present favorable reaction schemes that leads to efficient double molar intake of CO_2, with substantially barrierless reaction profiles.

In other AA anions, there is only on $—NH_2$ group and the second molecule has to react with the residual NH group which is, however, less active toward CO_2.

This second reaction for the simplest of the AA anion (glycinate) has to proceed through a sequence of isomerization reactions with a substantial energetic cost (15 kcal/mol). The reaction is nevertheless possible thereby providing a justification of the rather surprising molar intake measured for some ILs based on this simple anion.

The doubly deprotonated aspartate anion has a greater conformation mobility than glycinate and the second CO_2 molecule can be incorporated slightly more easily in the anion through a process which has a low activation barrier of about 6-7 kcal/mol.

In conclusion, we have shown that different AA anions do provide an efficient and effective absorbent of CO_2 molecules with sufficiently high molar intakes and that optimization of the environmental conditions such as counterion, temperature, viscosity might further increase the overall CO_2 intake to a degree which might be considered for practical applications.

In principle, the reactions explored here are reversible and could lead to the decarboxylation of the carbamates, hence in CO_2 desorption from the liquid. In general, the absorption of the first CO_2 molecule is largely exothermic, so that the decarboxylation of the carbamate would be thermodynamically hindered by about 20 kcal/mol for AA anions such as Gly, Lys and DAP and by even more for Asp. The reactions for the absorption of the second CO_2 molecule, however, are much less exothermic for most of the mechanisms considered here with ΔH typically around -12/-15 kcal/mol. It thus turns out that the products emerging from the intake of the second CO_2 molecule are less stable toward decarboxylation when compared to those arising from the absorption of the first one.

Acknowledgements

References

(1)   Stern, N. *The Economics of Climate Change: The Stern Review*; Cambridge University Press: Cambridge, 2007.
(2)   Meinshausen, M.; Meinshausen, N.; Hare, W.; Raper, S. C. B.; Frieler, K.; Knutti, R.; Frame, D. J.; Allen, M. R. Greenhouse-Gas Emission Targets for Limiting Global Warming to 2 °C. *Nature* **2009**, *458*, 1158–1162.
(3)   *Climate Change 2014: Synthesis Report*; Pachauri, R. K., Mayer, L., Eds.; IPCC: Geneva, Switzerland, 2015.
(4)   *IPCC Special Report on Carbon Dioxide Capture and Storage*; Metz, B., O. Davidson, H. C. de Coninck, M. Loos, and L. A. Meyer, Eds.; Cambridge University Press: Cambridge, 2005.
(5)   Figueroa, J. D.; Fout, T.; Plasynski, S.; McIlvried, H.; Srivastava, R. D. Advances in CO_2 Capture Technology—The U.S. Department of Energy's Carbon Sequestration Program. *Int. J. Greenh. Gas Control* **2008**, *2*, 9–20.

(6)   MacDowell, N.; Florin, N.; Buchard, A.; Hallett, J.; Galindo, A.; Jackson, G.; Adjiman, C. S.; Williams, C. K.; Shah, N.; Fennell, P. An Overview of CO_2 Capture Technologies. *Energy Environ. Sci.* **2010**, *3*, 1645.

(7)   *Materials for Carbon Capture*, 1st ed.; Jiang, D., Mahurin, S. M., Dai, S., Eds.; Wiley, 2020.

(8)   Rochelle, G. T. Amine Scrubbing for CO2 Capture. *Science* **2009**, *325*, 1652–1654.

(9)   Hsu, C. H.; Chu, H.; Cho, C. M. Absorption and Reaction Kinetics of Amines and Ammonia Solutions with Carbon Dioxide in Flue Gas. *J. Air Waste Manag. Assoc.* **2003**, *53*, 246–252.

(10)   Rao, A. B.; Rubin, E. S. A Technical, Economic, and Environmental Assessment of Amine-Based CO_2 Capture Technology for Power Plant Greenhouse Gas Control. *Environ. Sci. Technol.* **2002**, *36*, 4467–4475.

(11)   Cadena, C.; Anthony, J. L.; Shah, J. K.; Morrow, T. I.; Brennecke, J. F.; Maginn, E. J. Why Is CO_2 So Soluble in Imidazolium-Based Ionic Liquids? *J. Am. Chem. Soc.* **2004**, *126*, 5300–5308.

(12)   Gurkan, B.; Goodrich, B. F.; Mindrup, E. M.; Ficke, L. E.; Massel, M.; Seo, S.; Senftle, T. P.; Wu, H.; Glaser, M. F.; Shah, J. K.; Maginn, E. J.; Brennecke, J. F.; Schneider, W. F. Molecular Design of High Capacity, Low Viscosity, Chemically Tunable Ionic Liquids for CO_2 Capture. *J. Phys. Chem. Lett.* **2010**, *1*, 3494–3499.

(13)   Babamohammadi, S.; Shamiri, A.; Aroua, M. K. A Review of CO2 Capture by Absorption in Ionic Liquid-Based Solvents. *Rev. Chem. Eng.* **2015**, *31*.

(14)   Farsi, M.; Soroush, E. Chapter 4 - CO2 Absorption by Ionic Liquids and Deep Eutectic Solvents. In *Advances in Carbon Capture*; Rahimpour, M. R., Farsi, M., Makarem, M. A., Eds.; Woodhead Publishing, 2020; pp 89–105.

(15)   Wu, Y.; Xu, J.; Mumford, K.; Stevens, G. W.; Fei, W.; Wang, Y. Recent Advances in Carbon Dioxide Capture and Utilization with Amines and Ionic Liquids. *Green Chem. Eng.* **2020**, *1*, 16–32.

(16)   Earle, M. J.; Seddon, K. R. Ionic Liquids. Green Solvents for the Future. *Pure Appl. Chem.* **2000**, *72*, 1391–1398.

(17)   Brennecke, J. F.; Maginn, E. J. Ionic Liquids: Innovative Fluids for Chemical Processing. *AIChE J.* **2001**, *47*, 2384–2389.

(18)   Bates, E. D.; Mayton, R. D.; Ntai, I.; Davis, J. H. CO_2 Capture by a Task-Specific Ionic Liquid. *J. Am. Chem. Soc.* **2002**, *124*, 926–927.

(19)   Camper, D.; Bara, J. E.; Gin, D. L.; Noble, R. D. Room-Temperature Ionic Liquid–Amine Solutions: Tunable Solvents for Efficient and Reversible Capture of CO_2. *Ind. Eng. Chem. Res.* **2008**, *47*, 8496–8498.

(20)   Zhang, J.; Zhang, S.; Dong, K.; Zhang, Y.; Shen, Y.; Lv, X. Supported Absorption of CO2 by Tetrabutylphosphonium Amino Acid Ionic Liquids. *Chem. - Eur. J.* **2006**, *12*, 4021–4026.

(21)   Gurkan, B. E.; de la Fuente, J. C.; Mindrup, E. M.; Ficke, L. E.; Goodrich, B. F.; Price, E. A.; Schneider, W. F.; Brennecke, J. F. Equimolar CO_2 Absorption by Anion-Functionalized Ionic Liquids. *J. Am. Chem. Soc.* **2010**, *132*, 2116–2117.

(22)   Goodrich, B. F.; de la Fuente, J. C.; Gurkan, B. E.; Zadigian, D. J.; Price, E. A.; Huang, Y.; Brennecke, J. F. Experimental Measurements of Amine-Functionalized Anion-Tethered Ionic Liquids with Carbon Dioxide. *Ind. Eng. Chem. Res.* **2011**, *50*, 111–118.

(23)   Huang, Y.; Cui, G.; Wang, H.; Li, Z.; Wang, J. Absorption and Thermodynamic Properties of CO_2 by Amido-Containing Anion-Functionalized Ionic Liquids. *RSC Adv.* **2019**, *9*, 1882–1888.

(24) Le Donne, A.; Bodo, E. Cholinium Amino Acid-Based Ionic Liquids. *Biophys. Rev.* **2021**.

(25) Gontrani, L. Choline-Amino Acid Ionic Liquids: Past and Recent Achievements about the Structure and Properties of These Really "Green" Chemicals. *Biophys. Rev.* **2018**, *10*, 873–880.

(26) Gomes, J. M.; Silva, S. S.; Reis, R. L. Biocompatible Ionic Liquids: Fundamental Behaviours and Applications. *Chem. Soc. Rev.* **2019**, *48*, 4317–4335.

(27) Morandeira, L.; Álvarez, M. S.; Markiewicz, M.; Stolte, S.; Rodríguez, A.; Sanromán, M. Á.; Deive, F. J. Testing True Choline Ionic Liquid Biocompatibility from a Biotechnological Standpoint. *ACS Sustain. Chem. Eng.* **2017**, *5*, 8302–8309.

(28) Moshikur, R.; Chowdhury, R.; Moniruzzaman, M.; Goto, M. Biocompatible Ionic Liquids and Their Applications in Pharmaceutics. *Green Chem.* **2020**, *22*, 8116–8139.

(29) Goodrich, B. F.; de la Fuente, J. C.; Gurkan, B. E.; Lopez, Z. K.; Price, E. A.; Huang, Y.; Brennecke, J. F. Effect of Water and Temperature on Absorption of CO_2 by Amine-Functionalized Anion-Tethered Ionic Liquids. *J. Phys. Chem. B* **2011**, *115*, 9140–9150.

(30) Saravanamurugan, S.; Kunov-Kruse, A. J.; Fehrmann, R.; Riisager, A. Amine-Functionalized Amino Acid-Based Ionic Liquids as Efficient and High-Capacity Absorbents for CO_2. *ChemSusChem* **2014**, *7*, 897–902.

(31) Liu, A.-H.; Ma, R.; Song, C.; Yang, Z.-Z.; Yu, A.; Cai, Y.; He, L.-N.; Zhao, Y.-N.; Yu, B.; Song, Q.-W. Equimolar CO_2 Capture by N-Substituted Amino Acid Salts and Subsequent Conversion. *Angew. Chem. Int. Ed.* **2012**, *51*, 11306–11310.

(32) Onofri, S.; Adenusi, H.; Le Donne, A.; Bodo, E. CO_2 Capture in Ionic Liquids Based on Amino Acid Anions With Protic Side Chains: A Computational Assessment of Kinetically Efficient Reaction Mechanisms. *ChemistryOpen* **2020**, *9*, 1153–1160.

(33) Sistla, Y. S.; Khanna, A. CO2 Absorption Studies in Amino Acid-Anion Based Ionic Liquids. *Chem. Eng. J.* **2015**, *273*, 268–276.

(34) Hussain, M. A.; Soujanya, Y.; Sastry, G. N. Evaluating the Efficacy of Amino Acids as CO_2 Capturing Agents: A First Principles Investigation. *Environ. Sci. Technol.* **2011**, *45*, 8582–8588.

(35) Firaha, D. S.; Kirchner, B. Tuning the Carbon Dioxide Absorption in Amino Acid Ionic Liquids. *ChemSusChem* **2016**, *9*, 1591–1599.

(36) Shaikh, A. R.; Karkhanechi, H.; Kamio, E.; Yoshioka, T.; Matsuyama, H. Quantum Mechanical and Molecular Dynamics Simulations of Dual-Amino-Acid Ionic Liquids for CO_2 Capture. *J. Phys. Chem. C* **2016**, *120*, 27734–27745.

(37) Mercy, M.; de Leeuw, N. H.; Bell, R. G. Mechanisms of CO_2 Capture in Ionic Liquids: A Computational Perspective. *Faraday Discuss.* **2016**, *192*, 479–492.

(38) Gorantla, K. R.; Mallik, B. S. Reaction Mechanism and Free Energy Barriers for the Chemisorption of CO_2 by Ionic Entities. *J. Phys. Chem. A* **2020**, *124*, 836–848.

(39) Shaikh, A. R.; Ashraf, M.; AlMayef, T.; Chawla, M.; Poater, A.; Cavallo, L. Amino Acid Ionic Liquids as Potential Candidates for CO2 Capture: Combined Density Functional Theory and Molecular Dynamics Simulations. *Chem. Phys. Lett.* **2020**, *745*, 137239.

(40) Sheridan, Q. R.; Schneider, W. F.; Maginn, E. J. Role of Molecular Modeling in the Development of CO_2–Reactive Ionic Liquids. *Chem. Rev.* **2018**, *118*, 5242–5260.

(41) Luo, X. Y.; Fan, X.; Shi, G. L.; Li, H. R.; Wang, C. M. Decreasing the Viscosity in CO_2 Capture by Amino-Functionalized Ionic Liquids through the Formation of Intramolecular Hydrogen Bond. *J. Phys. Chem. B* **2016**, *120*, 2807–2813.

(42) Li, F.; Bai, Y.; Zeng, S.; Liang, X.; Wang, H.; Huo, F.; Zhang, X. Protic Ionic Liquids with Low Viscosity for Efficient and Reversible Capture of Carbon Dioxide. *Int. J. Greenh. Gas Control* **2019**, *90*, 102801.

(43) Chen, F.-F.; Huang, K.; Zhou, Y.; Tian, Z.-Q.; Zhu, X.; Tao, D.-J.; Jiang, D.; Dai, S. Multi-Molar Absorption of CO_2 by the Activation of Carboxylate Groups in Amino Acid Ionic Liquids. *Angew. Chem. Int. Ed.* **2016**, *55*, 7166–7170.

(44) Chen, X.; Luo, X.; Li, J.; Qiu, R.; Lin, J. Cooperative CO2 Absorption by Amino Acid-Based Ionic Liquids with Balanced Dual Sites. *RSC Adv.* **2020**, *10*, 7751–7757.

(45) Prakash, P.; Venkatnathan, A. Site-Specific Interactions in CO_2 Capture by Lysinate Anion and Role of Water Using Density Functional Theory. *J. Phys. Chem. C* **2018**, *122*, 12647–12656.

(46) Luo, X. Y.; Lv, X. Y.; Shi, G. L.; Meng, Q.; Li, H. R.; Wang, C. M. Designing Amino-Based Ionic Liquids for Improved Carbon Capture: One Amine Binds Two CO_2. *AIChE J.* **2019**, *65*, 230–238.

(47) Li, C.; Lu, D.; Wu, C. Multi-Molar CO_2 Capture beyond the Direct Lewis Acid–Base Interaction Mechanism. *Phys. Chem. Chem. Phys.* **2020**, *22*, 11354–11361.

(48) Grimme, S.; Antony, J.; Ehrlich, S.; Krieg, H. A Consistent and Accurate *Ab Initio* Parametrization of Density Functional Dispersion Correction (DFT-D) for the 94 Elements H-Pu. *J. Chem. Phys.* **2010**, *132*, 154104.

(49) Frisch, M. J.; Trucks, G. W.; Schlegel, H. B.; Scuseria, G. E.; Robb, M. A.; Cheeseman, J. R.; Scalmani, G.; Barone, V.; Petersson, G. A.; Nakatsuji, H.; et al. *Gaussian 16 Rev. C.01*; Wallingford, CT, 2016.

(50) Marenich, A. V.; Cramer, C. J.; Truhlar, D. G. Universal Solvation Model Based on Solute Electron Density and on a Continuum Model of the Solvent Defined by the Bulk Dielectric Constant and Atomic Surface Tensions. *J. Phys. Chem. B* **2009**, *113*, 6378–6396.

(51) Bennett, E. L.; Song, C.; Huang, Y.; Xiao, J. Measured Relative Complex Permittivities for Multiple Series of Ionic Liquids. *J. Mol. Liq.* **2019**, *294*, 111571.

TOC graphic